

Noise Transmission Characteristics of Advanced Composite Structural Materials

Louis A. Roussos* and Clemans A. Powell†
NASA Langley Research Center, Hampton, Virginia
 Ferdinand W. Grosveld‡
Bionetics Corporation, Hampton, Virginia
 and
 Leslie R. Koval§
University of Missouri-Rolla, Rolla, Missouri

An experimental and theoretical research program has begun to develop an understanding of the noise transmission characteristics of composite materials. Such an understanding will ensure that the weight advantage of composites in aircraft fuselage design is not compromised by high noise transmission or heavy acoustic treatments. Noise transmission tests have been conducted on large unstiffened panels representative of the outer skin or inner trim panels of aircraft fuselages. Also, an analytical model based on infinite panel theory has been developed which allows for exact modeling of the anisotropic properties of the panels.

In the mass controlled and coincidence frequency regions, agreement between the measured and analytical noise transmission loss was quite good. A theoretical design comparison between aluminum and composite general aviation panels based on equal critical shear load showed the graphite/epoxy and Kevlar[®]/epoxy panels to have 3 to 4 dB less transmission loss than an aluminum panel over most of the frequency range due to their lighter weight and 6 to 12 dB less transmission loss at high frequency because of their lower critical frequencies.

A finite panel field incidence transmission loss theory has also been developed. Preliminary calculations for oblique incidence transmission loss indicate that improved low frequency transmission loss may be possible with composites relative to conventional aluminum panels.

Nomenclature

A	= absorption area, m ²
A_{eq}	= equivalent absorption area, m ²
ALUM	= aluminum
c	= speed of sound in air, m/s
D_{11} D_{12} D_{16}	= anisotropic plate rigidities, N m
D_{22} D_{26}	
E	= Young's modulus, Pa
E_{11} E_{22}	= orthotropic elastic moduli in a composite tape ply parallel and perpendicular to the fibers respectively, Pa
f	= frequency, Hz
f_{coinc}	= coincidence frequency, Hz
f_{crit}	= critical frequency, Hz
f_L	= lower frequency of a one third octave band, Hz
f_U	= upper frequency of a one third octave band Hz
F/E	= fiberglass epoxy
G	= isotropic plate shear modulus Pa
G_{12}	= shear modulus for composite tape ply, Pa
G/E	= graphite/epoxy
h	= panel thickness, cm
j	= $\sqrt{-1}$
k	= integer designating the k th layer of a composite panel

k_x	= wave number in x direction = $(2\pi f \sin \theta_i \cos \phi_i)/c$, m ⁻¹
k_y	= wave number in y direction = $(2\pi f \sin \theta_i \sin \phi_i)/c$, m ⁻¹
K/E	= Kevlar [®] /epoxy
\bar{m}	= mass per unit area kg/m ²
N	= number of layers in composite panel
NR	= noise reduction, dB
p	= pressure, Pa
P_i	= amplitude of an incident pressure wave Pa
P_t	= amplitude of a transmitted pressure wave, Pa
\bar{Q}_{ij}	= the reduced stiffnesses relating stress to strain in a composite ply, Pa
S	= surface area, m ²
$S(f)$	= power spectral density of the incident pressure at frequency f , Pa ² /Hz
t	= time, s
TL	= transmission loss dB
TL_{ML}	= field incidence mass law transmission loss, dB
w	= plate displacement m
X Y Z	= panel coordinate axes
x y z	= displacement along respective axes, m
z_k	= z direction distance from panel middle surface to bottom of the k th layer (see Fig. 4) m
Δf	= narrow frequency bandwidth, Hz
η	= damping loss factor
θ	= angle of fiber direction to a specified boundary axis of the panel deg
θ_i	= the angle of incident pressure wave relative to the Z axis (the axis normal to the panel), deg
ν	= isotropic plate Poisson's ratio
ν_{12} ν_{21}	= composite tape ply Poisson's ratios

Presented as Paper 83 0694 at the AIAA 8th Aeroacoustics Conference Atlanta Ga April 11 13 1983; received July 11 1983; revision received Feb 9 1984. This paper is declared a work of the U.S. Government and therefore is in the public domain.

*Aerospace Technologist

†Head Structural Acoustics Branch

‡Aerospace Research Engineer Member AIAA

§Professor Mechanical Engineering Member AIAA

¶Kevlar is a registered trademark for an aramid fiber produced by E. I. DuPont de Nemours & Co.

ρ	= mass density of air, kg/m ³
τ	= transmission coefficient
$\bar{\tau}$	= field incidence transmission coefficient
ϕ_i	= angle of incident pressure wave relative to the X axis of the panel when projected into the plane of the panel deg

Introduction

THE noise transmission characteristics of composite materials have been identified as a principal design consideration for aircraft with composite fuselages.¹ These characteristics must be taken into account early in the design process to ensure that the weight saving advantage of composite construction is not compromised by high noise transmission which would necessitate heavy add on acoustic treatments.² Studies of noise transmission of composites, either experimental or theoretical have been limited in both number and scope. The experimental study of Yang and Tsui³ considered only three panels and was conducted in a small facility with a usable frequency range of 400 Hz to 10 kHz. The theoretical study by Revell, et al.² investigated the effects of high stiffness, low-mass isotropic materials on noise transmission, rather than effects of actual composite type materials.

The theoretical study by Koval,⁴ which provided the first model for noise transmission loss of composite constructions was for an infinite monocoque cylindrical shell. This study was limited to a few configurations, was not substantiated by experimental data, and compared aluminum and composite configurations only for conditions of equal mass.

The NASA Langley Research Center has begun a theoretical and experimental program to provide the necessary noise transmission information for composite structures so that these characteristics can be incorporated early in design phases for weight efficient aircraft structures. The objective of the first phase of this program is to determine how composite structures will affect fuselage noise transmission relative to current aluminum structures. This paper presents the results of a theoretical and experimental study of noise transmission of large unstiffened panels representative of aircraft outer skins and interior trim which was conducted to meet this objective.

Description of Experimental Method

To establish the noise transmission loss characteristics of the composite test panels experimentally, the panels were mounted as partitions between two adjacent rooms, designated as source room and receiving room. Top and side views of the transmission loss apparatus are shown in Fig. 1. In the source room, which measures 3.35 by 3.66 by 3.94 m, a diffuse field was established by two reference sound power sources. Sound is transmitted from the source room into the receiving room only by way of the test panel which has a sound exposed vibrating area of 0.85 by 1.46 m. The test specimen is mounted in a steel frame which is designed for minimum structural flanking. The receiving room, with dimensions of 4.47 by 3.36 by 2.90 m, is acoustically and structurally isolated from the rest of the building. A space and time average of the sound pressure levels is taken in each of the rooms by a microphone mounted at the end of a rotating boom. The noise reduction (NR), defined as the difference between the measured averaged sound pressure levels in the source and receiving rooms, includes characteristics of the test specimen as well as room characteristics. The classical method⁵ of measuring transmission loss assumes that the sound pressure levels are measured in a diffuse field in both the source and receiving rooms. By correcting for the room characteristics using the measured absorption area A of the receiving room, the noise transmission loss (TL) which is a function of the properties of only the test specimen, can be

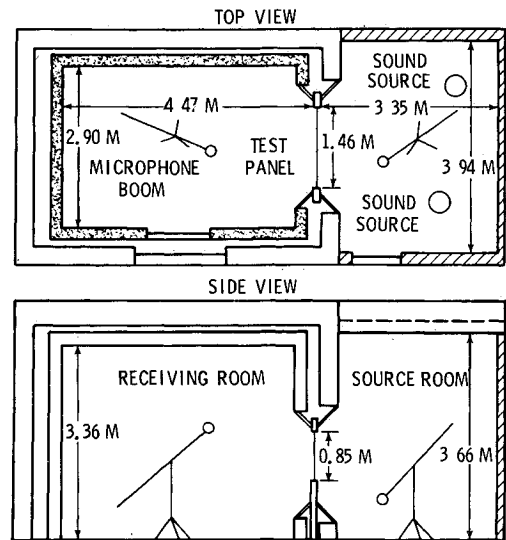


Fig. 1 Top and side views of transmission loss apparatus

calculated by

$$TL = NR + 10 \log (S/A) \quad (1)$$

where S is the surface area of the test specimen. The underlying assumptions for this technique are not applicable for the present setup in the low frequency region (below 500 Hz) due to the large wavelength of sound relative to the dimensions of the rooms and microphone booms. In Ref. 6 the "plate reference method" is suggested to measure the TL more accurately in a frequency range 100 Hz to 10 kHz. This method not only corrects the noise reduction for the absorption in the receiving room but also corrects for the nondiffusivity of both rooms by assuming a mass law type of behavior of the reference panel.

With the plate reference method Eq. (1) is rewritten as

$$TL = NR + 10 \log (S/A_{eq}) \quad (2)$$

where A_{eq} is an equivalent absorption area. Assuming that TL follows field incidence mass law, Eq. (2) can be solved for A_{eq} .

$$A_{eq} = S \times 10^{(NR - TL_{ML})/10} \quad (3)$$

TL_{ML} is the field incidence mass law transmission loss given by

$$TL_{ML} = 10 \log \left[\frac{\left(0.978 \frac{\bar{m} \pi f}{\rho c} \right)^2}{\ln \left[\frac{1 + \left(\frac{\bar{m} \pi f}{\rho c} \right)^2}{1 + \left(0.208 \frac{\bar{m} \pi f}{\rho c} \right)^2} \right]} \right] \quad (4)$$

where ρc is the characteristic impedance of air. The derivation of Eq. (4) is given in Ref. 7. The equivalent absorption area A_{eq} is dependent on frequency and may be used strictly as a correction factor for only one particular test setup and room configuration. Practically the A_{eq} measured for the reference panel is good for a variety of test panels since the panel

surface area is small compared to the total area of the receiving room. The repeatability of transmission loss tests using this method is very good as the accuracy between tests is within tenths of a dB.⁶ A 3.18 mm thick rubber reference panel was used to determine A_{eq} for this test series. It is expected to follow the field incidence mass law over the frequency range of interest (100 Hz to 10 kHz) because it has a calculated resonant frequency of 0.2 Hz (simply supported edge conditions) and a critical frequency of approximately 3×10^5 Hz, both of which are far outside the frequency region of interest.

Description of Test Panels

A total of 14 fiber reinforced composite panels were tested. Ten of these panels were of tape construction, two were of fabric construction, and two were of sandwich construction with fabric composite skins and microballoon filled epoxy cores. The panels of tape construction were made by bonding several plies of unidirectional fibers. Each ply (see Fig. 2) consists of bundles of high strength fibers, all lying in one direction and held together by an epoxy resin giving the appearance of a strip of tape (hence "tape construction"). The plies were formed by cutting the tape strips so that each ply had the desired fiber direction with respect to the boundaries of the panel. For example, a 0 or 90 deg ply has its fiber direction parallel to one of the panel boundaries, while a 45 deg ply has its fibers running in a direction that forms a 45 deg angle with one of the boundaries. The composite panels were then formed by bonding together several plies of various angles usually in a manner called "balanced symmetric" where the ply angles are symmetric about the mid plane of the panel and every ply angle is balanced by another ply at the negative of that angle. All the tape panels in the present tests were balanced symmetrically. Three different types of fiber/epoxy panels were tested: graphite/epoxy (G/E), Kevlar/epoxy (K/E), and fiberglass/epoxy (F/E). The panels were 0.91 m long and 1.52 m wide and had thicknesses of about 0.1 and 0.2 cm. The boundary along the long dimension

of the panel was chosen as the 0 deg direction. The designation given to each tape panel for future reference and details on the ply angles, thickness, and surface density for these panels are presented in Table 1. The fiber orientations listed in the table are for one half the panel thickness, i.e., from one surface to the mid plane. The remaining plies are in reverse order from the mid plane to the other surface. The panels with fabric construction were similarly made by bonding several plies together. However, instead of having unidirectional fibers in a resin matrix, a fabric ply consists of bundles of fibers woven together perpendicular to each other. In what is called the "fill direction," the fibers are straight (i.e., unbent), while in the opposite "warp direction" the fibers bend up and down as they weave around the fill direction fibers (see Fig. 3). As with the tape panels, the fabric panels were all balanced symmetrically. Only G/E fabric panels were constructed in time for the present study. All the fabric plies were cut so that the warp direction was parallel to the long dimension of the panel. The designation, thickness, and surface density for the fabric panels and the sandwich panels (which had fabric skins) are presented in Table 1.

Infinite Panel Theory Transmission Loss Model

Using classical thin plate theory, the equation of motion governing the bending vibrations of a symmetrically layered composite panel is⁸

$$D_{11} w_{xxxx} + 4D_{16} w_{xxxy} + 2(D_{12} + 2D_{66}) w_{xxyy} + 4D_{26} w_{xyyy} + D_{22} w_{yyyy} + \bar{m} w_{tt} = p(x, y, t) \quad (5)$$

where a comma denotes the partial differentiation with respect to the subscript and the D_{ij} terms are the anisotropic plate rigidity values that relate the internal bending and twisting moments of the plate to the twists and curvatures

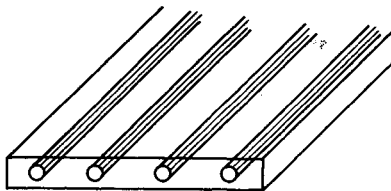


Fig. 2 Details of tape ply construction

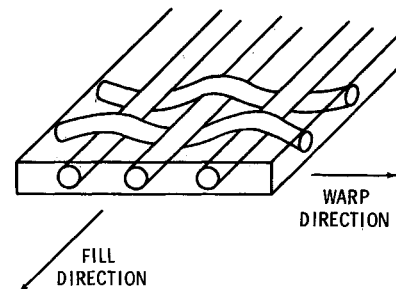


Fig. 3 Details of fabric ply construction

Table 1 Description of panels

Panel designation	Fiber material	Fiber orientation deg	No of plies	Thickness, cm	Surface density, kg/m ²
GT1	Graphite tape	45/-45/45/-45	8	0.102	1.59
GT2	Graphite tape	0/90/0/90	8	0.102	1.59
GT3	Graphite tape	45/-45/45/-45	16	0.185	3.05
		45/-45/45/-45			
KT1	Kevlar tape	45/-45/45/-45	8	0.102	1.37
KT2	Kevlar tape	0/90/0/90	8	0.102	1.37
KT3	Kevlar tape	45/-45/45/-45	16	0.203	2.79
		45/-45/45/-45			
KT4	Kevlar tape	0/90/45/-45	16	0.203	2.79
		0/90/45/-45			
FT1	Fiberglass tape	45/-45/45/-45	8	0.102	2.21
FT2	Fiberglass tape	0/90/0/90	8	0.102	2.18
FT3	Fiberglass tape	45/-45/45/-45	16	0.201	4.70
		45/-45/45/-45			
GF1	Graphite fabric		3	0.109	1.64
GF2	Graphite fabric		6	0.211	3.31
GF3	Graphite fabric		6	0.318 (0.10 core)	4.16
GF4	Graphite fabric		6	0.418 (0.20 core)	4.82

they induce For an isotropic plate, $D_{11} = D_{22} = Eh^3 / [12(1 - \nu^2)]$, $D_{12} = \nu D_{11}$, $D_{66} = Gh^3/12$, and because twisting behavior is uncoupled from bending behavior, $D_{16} = D_{26} = 0$. For an orthotropic plate, D_{11} no longer equals D_{22} , but again, $D_{16} = D_{26} = 0$. Many composite panels, however, are governed by anisotropic behavior where D_{16} and D_{26} are nonzero, which means that the bending and twisting moments are coupled to the twists and curvatures, respectively.

D_{ij} for Tape Panels

The theory for calculating the flexural rigidities D_{ij} for tape panels is well established and documented.⁸ Each ply is modelled as an orthotropic layer with the following properties:

- E_{11} = modulus of elasticity in direction parallel to fibers
- E_{22} = modulus of elasticity in direction perpendicular to fibers
- ν_{12} = ratio of strains perpendicular and parallel to stress where the stress is parallel to fibers
- G_{12} = shear modulus
- $\nu_{21} = E_{22}/E_{11} \nu_{12}$

The properties of each ply and the angle of orientation θ of the fibers in each ply are used to calculate the flexural rigidities from the following equation⁸:

$$D_{ij} = \frac{1}{3} \sum_{k=1}^N (\bar{Q}_{ij})_k (z_k^3 - z_{k-1}^3)$$

where z_k is the z direction distance from the middle surface to the bottom of the k th layer (see Fig. 4), and $(\bar{Q}_{ij})_k$ are the reduced stiffnesses for the k th layer that relate the stresses in that layer to the strains. The \bar{Q}_{ij} are a function of E_{11} , E_{22} , ν_{22} , G_{12} , and θ . The derivation of the equations for \bar{Q}_{ij} is straightforward and given in Ref. 8. A ply that has its fibers parallel to one of the panel boundaries, either $\theta = 0$ or 90 deg, will behave orthotropically. However, for all other θ values, the ply will behave anisotropically. Therefore, unless the panel is made up of plies that are either all 0 deg, all 90 deg, or all 0 and 90 deg, the panel will behave anisotropically. From Table 1, most of the panels are seen to be anisotropic. For the case of "many" layers, Ref. 8 indicates that D_{16} and D_{26} are

small compared to the other rigidity values so that orthotropic analysis may be used; but care should be taken in calculating critical loads because in that case even small values of D_{16} and D_{26} can have a significant effect.

Estimated stiffness properties from design guides, company brochures, etc., were used in the analytical model predictions. Table 2 presents the ply properties, i.e., E_{11} , E_{22} , ν_{12} , and G_{12} that were used for each material. In Table 3, the calculated D_{ij} values are given for each of the ten tape panels. The angle layup is seen to have a significant effect on D_{ij} . Thus, as will be discussed later, angle layup has an important effect on the resonant frequency of a panel. Also, note that judging whether D_{16} and D_{26} are small compared to the other rigidities is not necessarily a simple decision.

D_{ij} for Fabric Panels

The theory for calculating the flexural rigidities D_{ij} for fabric panels is neither well established nor documented. Because each ply consists of a weave of fibers, each ply may be anisotropic in behavior, whereas a ply of a tape panel is orthotropic in behavior when the principal axes are ap-

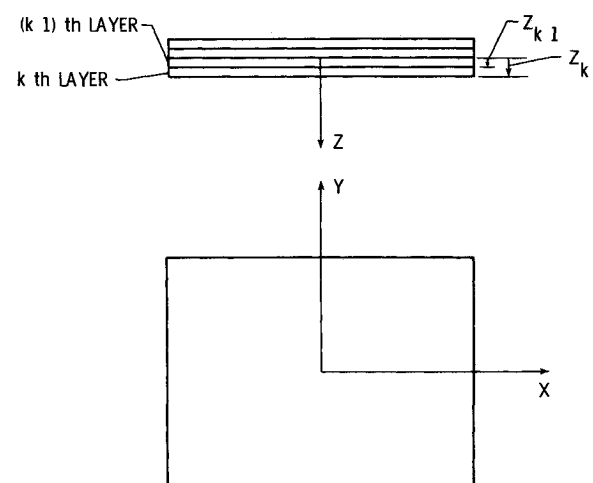


Fig. 4 Panel geometry

Table 2 Ply properties for tape and fabric panels

Material	E_{11} , Pa	E_{22} , Pa	ν_{12}	G_{12} , Pa	Density, kg/m ³
Graphite tape	13.7×10^{10}	1.0×10^{10}	0.30	0.5×10^{10}	1.55×10^3
Kevlar tape	7.6×10^{10}	0.6×10^{10}	0.34	0.2×10^{10}	1.36×10^3
Fiberglass tape	3.9×10^{10}	0.9×10^{10}	0.30	0.2×10^{10}	2.19×10^3
Graphite fabric	6.9×10^{10}	6.9×10^{10}	0.30	26.5×10^{10}	1.55×10^3
Core	0.7×10^{10}	0.7×10^{10}	0.30	4.1×10^{10}	0.89×10^3

Table 3 Rigidity values for tape and fabric panels

Panel	D_{11} , N m	D_{12} , N m	D_{16} , N m	D_{22} , N m	D_{26} , M n	D_{66} , M n
GT1	3.79	2.95	1.06	3.79	1.06	3.12
GT2	8.60	0.25	0.00	4.37	0.00	0.42
GT3	23.06	17.93	3.21	23.06	3.21	18.95
KT1	2.04	1.68	0.58	2.04	0.58	1.71
KT2	4.73	1.54	0.00	2.40	0.00	0.18
KT3	16.34	13.45	2.33	16.34	2.33	13.65
KT4	27.65	5.05	0.87	21.82	0.87	5.26
FT1	2.58	1.02	0.30	2.58	0.30	1.40
FT2	3.80	0.40	0.00	2.60	0.00	0.78
FT3	19.90	7.83	1.16	19.90	1.16	10.76
GF1	8.2	2.5	0.0	8.2	0.0	2.9
GF2	59.2	17.8	0.0	59.2	0.0	20.7
GF3	196.6	59.0	0.0	196.6	0.0	69.0
GF4	297.8	89.4	0.0	297.8	0.0	106.0

appropriately chosen. However, the only data available were estimates of equivalent orthotropic moduli. These are presented in Table 2. Also given in Table 2 are the estimated material properties of the microballoon filled epoxy core used in the sandwich panels. In Table 3, the calculated D_{ij} values are given for the fabric panels. If the actual ply properties are anisotropic, then the equations for the reduced stiffnesses \bar{Q}_{ij} given in Ref. 8 are not applicable and new equations for \bar{Q}_{ij} should be derived.

Transmission Loss Calculation

Transmission loss (TL) is given by

$$TL = 10 \log(1/\tau) \quad (6)$$

where τ is the transmission coefficient and defined by

$$\tau = \frac{\text{transmitted acoustic intensity}}{\text{incident acoustic intensity}} \quad (7)$$

The pressure $p(x, y, t)$ acting on the panel is the sum of the incident, reflected, and transmitted pressures. These pressures, along with the displacement of the plate $w(x, y, t)$, are assumed to be harmonic travelling waves. Because the pressures are modeled as plane waves, the equation for the transmission coefficient [Eq. (7)] reduces to

$$\tau = |P_t|^2 / |P_i|^2 \quad (8)$$

where P_t and P_i are the amplitudes of the transmitted and incident pressures. Forcing velocity to be continuous through the plate provides the two necessary boundary conditions so that Eq. (5) can be solved for the ratio of incident to transmitted pressure

$$\frac{P_t}{P_i} = 1 + \frac{\cos \theta_i}{j f \pi 4 \rho c} (1 + j \eta) \left[-\frac{\bar{m} 4 \pi^2 f^2}{1 + j \eta} + D_{11} k_x^4 + 4 D_{16} k_x^3 k_y + 2 (D_{12} + 2 D_{66}) k_x^2 k_y^2 + 4 D_{26} k_x k_y^3 + D_{22} k_y^4 \right] \quad (9)$$

Substituting Eq. (9) into Eq. (8) gives the transmission coefficient for oblique incidence transmission at a single frequency, whereas the tests are for field incidence transmission in one third octave bands. To calculate the field incidence transmission coefficient $\bar{\tau}$, the incident and transmitted intensities are each integrated over a hemispherical solid angle defined by θ_i and ϕ_i . Thus, writing $\bar{\tau}(f)$ in terms of $\tau(\theta_i, \phi_i, f)$ results in

$$\bar{\tau}(f) = \frac{\int_{\phi_i=0}^{2\pi} \int_{\theta_i=0}^{\theta_{LIM}} \tau(\theta_i, \phi_i, f) \cos \theta_i \sin \theta_i d\theta_i d\phi_i}{\int_{\phi_i=0}^{2\pi} \int_{\theta_i=0}^{\theta_{LIM}} \cos \theta_i \sin \theta_i d\theta_i d\phi_i} \quad (10)$$

where θ_{LIM} is commonly equated to 78 deg for field incidence transmission.

For predicting TL in one third octave bands, the incident and transmitted intensities must be summed within the bands. Thus, the TL for a one third octave band is given by⁷

$$TL = 10 \log \left[\sum_{f=f_L}^{f_U} S(f) \Delta f \right] / \left[\sum_{f=f_L}^{f_U} \bar{\tau}(f) S(f) \Delta f \right] \quad (11)$$

where $S(f)$ is the power spectral density of the incident pressure at frequency f with narrow frequency bandwidth Δf .

Coincidence Frequency and Critical Frequency

Investigating Eq. (9) for the case of no damping ($\eta=0$) reveals that for some particular frequency the term in brackets will be zero. At this frequency $\tau(\theta_i, \phi_i, f)$ will equal unity and TL will be zero, meaning that all the sound will be transmitted. This frequency is called "coincidence frequency" and is so named because at this frequency the trace wavelength of the sound wave on the panel is equal to the free bending wavelength of the panel. The actual TL at this frequency depends on how much damping is present in the panel. The equation for coincidence frequency is thus calculated to be

$$f_{\text{coinc}} = \frac{c^2}{2\pi \sin^2 \theta_i} \left\{ \bar{m} / [D_{11} \cos^4 \phi_i + 4 D_{16} \cos^3 \phi_i \sin \phi_i + 2 (D_{12} + 2 D_{66}) \cos^2 \phi_i \sin^2 \phi_i + 4 D_{26} \cos \phi_i \sin^3 \phi_i + D_{22} \sin^4 \phi_i] \right\}^{1/2} \quad (12)$$

The critical frequency, f_{crit} , is the lowest possible value of the coincidence frequency. From the above, the lowest value of f_{crit} relative to θ_i occurs where $\sin \theta_i$ is a maximum, that is, at $\theta_i = 78$ deg (maximum value of θ_i in field incidence TL calculation). However, the value of ϕ_i for minimizing f_{coinc} cannot be calculated *a priori*; therefore f_{crit} was found iteratively. Table 4 presents the calculated field incidence critical frequencies for all the composite test panels. The comparatively low critical frequencies for the sandwich panels indicate that highly stiffened panels can have dramatically reduced critical frequencies.

Results and Discussion

In Fig. 5 the measured TL of two graphite/epoxy tape panels is compared with field incidence mass law and with the infinite panel theory developed in the previous section. In Fig. 6 the measured TL of a sandwich panel is compared with infinite panel theory. These figures are discussed below in relation to the mass controlled and coincidence frequency regions.

Mass Controlled Frequency Region Comparison

In Fig. 5 field incidence mass law is seen to be in good agreement with the tape panel data (within 1 dB) over a wide frequency range. In general, the thicker (and stiffer) the panel, the lower the frequency at which the data deviates from mass law because of the lower critical frequency. For example, in Fig. 5, mass law agrees well with data up to 6300 Hz for the 0.102 cm panel (panel GT2 in Table 1) but only up to 2500 Hz for the 0.185 cm panel (GT3). For all panels, agreement was good down to 163 Hz. As expected, infinite panel theory agrees with mass law from the lowest frequency up to the point where coincidence effects become important, that is, where both the data and the infinite panel theory diverge from mass law.

Because the panels behaved in a mass law manner in the mass controlled region, the stiffness and, thus, the fiber orientations of the panel did not affect TL in this region.

Table 4 Calculated field incidence critical frequencies

Panel	Critical frequency, Hz	Panel	Critical frequency, Hz
GT1	8391	FT1	14902
GT2	8391	FT2	14902
GT3	4409	FT3	7862
KT1	10523	GF1	8835
KT2	10523	GF2	4621
KT3	5618	GF3	2867
KT4	6144	GF4	2173

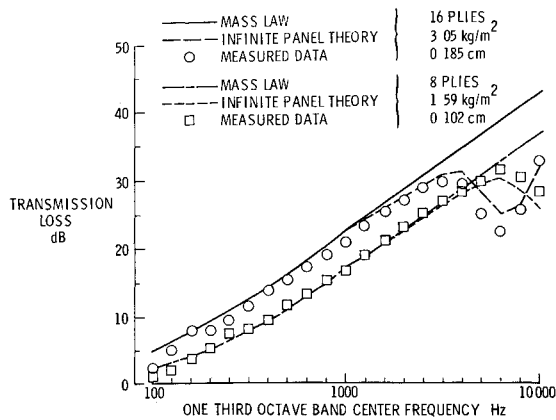


Fig 5 Transmission loss characteristics of graphite/epoxy panels, GT2 and GT3

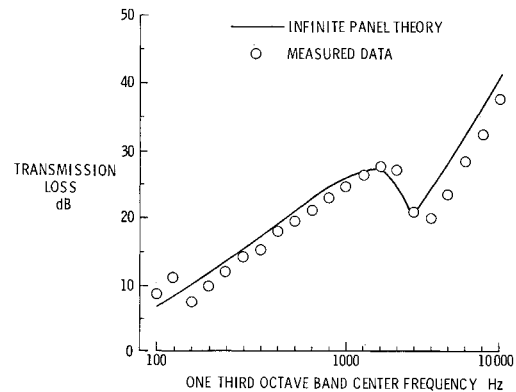


Fig 6 Transmission loss characteristics of graphite/epoxy fabric sandwich panel GF3 with 0.1 cm, microballoon filled epoxy core

Therefore, when comparing any two panels it is simply observed that the panel with the larger surface density will have the higher TL

Coincidence Frequency Region Comparison

The agreement between infinite panel theory and experimental data is quite good in the coincidence region. In Fig 5, the theory follows the slope of the coincidence dips for both graphite/epoxy panels and is within 1 to 3 dB of the levels. Similar results were found for the Kevlar/epoxy and fiberglass/epoxy panels.

The sandwich panels, which had G/E fabric skins and microballoon filled epoxy cores, had the lowest predicted critical frequencies and had the estimated stiffness values with the least level of confidence since they were assumed isotropic (see Tables 3 and 4). Still, as indicated in Fig 6 the theory does predict the shape and trend of the measured transmission loss in the coincidence region.

Several interesting comparisons can be made in studying Table 4. In comparing composite panels with equal thicknesses, the stiffer panel had the lower critical frequency. Thus the G/E panels have lower critical frequencies than the K/E panels, which in turn have lower critical frequencies than the F/E panels. On comparing panels with different thicknesses of the same composite material, the increased thickness is found to cause a greater increase in panel stiffness than in panel surface density so that the thicker panel has a lower critical frequency. Because of this, at high frequencies where the thicker panel enters its coincidence frequency region, the thinner lighter panel has significantly greater (5 to 9 dB) transmission loss. At even higher frequencies, the thicker panel again would have greater TL .

Although the ply angle layout had no effect on TL in the mass controlled region, it may effect the value of the critical frequency and the TL in the coincidence region. Based on infinite panel theory, a panel that is made of all 0/90 deg plies has the same coincidence region characteristics as a panel made of all 45/-45 deg plies. Therefore, the calculated frequencies (Table 4) are identical for both panels comprising the pairs GT1/GT2, KT1/KT2, and FT1/FT2. However, the 16 ply Kevlar panels, KT3/KT4, have different calculated critical frequencies because KT3 has all plies at 45/-45 deg, whereas KT4 has a mixture of 45/-45 deg and 0/90 deg plies. This difference in ply layout increased the calculated critical frequency for KT4 by 9% over that of KT3. This difference, as expected, was not detectable in the measured one third octave band transmission loss data.

Design Comparison of Composites and Aluminum

In this section, the effect on noise transmission of replacing a typical general aviation aluminum skin with either G/E

K/E or F/E skins is investigated. In designing a fuselage skin, the thickness of the skin panel is influenced by several design considerations, namely, impact damage tolerance and fatigue damage resistance and its fail safe capability to maintain flight safety in the event of structural damage.¹ The design comparison presented in this section is based on fatigue damage resistance. The criterion for resistance to fatigue damage essentially amounts to a restriction on the initial shear buckling strength of the skin. The design loads of composite material skins are not expected to be any different than those for an aluminum skin, therefore the design comparison presented here is based on equal critical shear load for the composite and aluminum panels. The panels were assumed to be sized 20.3 by 35.6 cm with simply supported boundary conditions. The composite panels were assumed to be of tape construction with each ply restricted to be 0.013 cm (0.005 in.) thick, which was the nominal ply thickness of the test panels. The critical shear load was first calculated for the aluminum panel which was assumed to have a 0.101 cm (0.040 in.) thick skin. A number of ply angle configurations were then investigated for each composite material so that the minimum thickness composite panel was found whose critical shear load either met or exceeded that of the aluminum panel. The critical shear loads were calculated using orthotropic theory.⁹ The ply angles and calculated rigidities of the design panels are given in Table 5, where it can be seen that D_{16} and D_{26} for the composite panels are about an order of magnitude less than the other rigidity values. With the panels thus designed, the infinite panel noise transmission theory developed earlier in this paper was used to calculate the transmission loss of the panels. These results are presented in Fig 7. The F/E panel has slightly greater TL than the aluminum panel because its design weight is slightly greater. The G/E and K/E panels have design weights about 35 and 33%, respectively lighter than aluminum and thus have about 3 to 4 dB less transmission loss over their mass controlled regions. At the highest frequencies of comparison, the G/E and K/E have 6 to 12 dB less TL than the aluminum panel because the G/E and K/E panels have lower critical frequencies.

In the low frequency, stiffness controlled transmission loss region, high stiffness composites might provide increased transmission loss compared to aluminum. This topic is discussed in the following analytical section.

Stiffness Controlled TL and Finite Panel Analysis

To investigate the effects of high strength/lightweight composites in the low frequency region of transmission loss, experimental studies are planned for small panels with fundamental frequencies of typically 100 Hz or more. In order to calculate the transmission loss of these panels at or near resonance the analytical model must take into account

Table 5 Description of design comparison panels

Material	Fiber orientations, deg	Rigidity values N m						Surface density kg/m ²
		D_{11}	D_{12}	D_{16}	D_{22}	D_{26}	D_{66}	
Aluminum	N A	6 78	2 26	0 00	6 78	0 0	2 32	2 81
Graphite/epoxy	45/-45/0/90/0 90/0/-45/45	6 86	3 54	0 93	5 26	0 93	3 78	1 78
Kevlar/epoxy	45/45/90/0/90/0/ 90/0/90/-45/45	5 45	3 35	0 66	7 21	0 66	3 41	1 89
Fiberglass/epoxy	45/-45/90/0/90/0/ 90/0/90/-45/45	6 43	2 15	0 33	7 31	0 33	3 11	3 00

Table 6 Calculated fundamental resonance frequencies for test panels

Panel	Frequency Hz		Panel	Frequency Hz	
	Simply Supported	Clamped		Simply Supported	Clamped
GT1	6 0	9 9	FT1	3 6	6 4
GT2	4 3	9 2	FT2	3 1	6 1
GT3	10 6	17 9	FT3	6 9	12 6
KT1	4 8	7 9	GF1	6 4	12 5
KT2	3 4	7 3	GF2	12 3	23 9
KT3	9 2	15 5	GF3	19 8	38 5
KT4	8 0	15 9	GF4	26 2	50 8
Aluminum 0 082 cm	3.6	7 0	Aluminum 0 161 cm	7 2	13 9

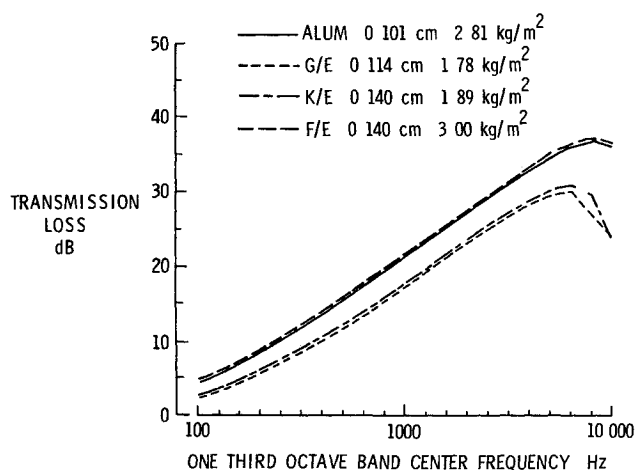


Fig 7 Infinite panel theory transmission loss for design comparison of aluminum and composite panels

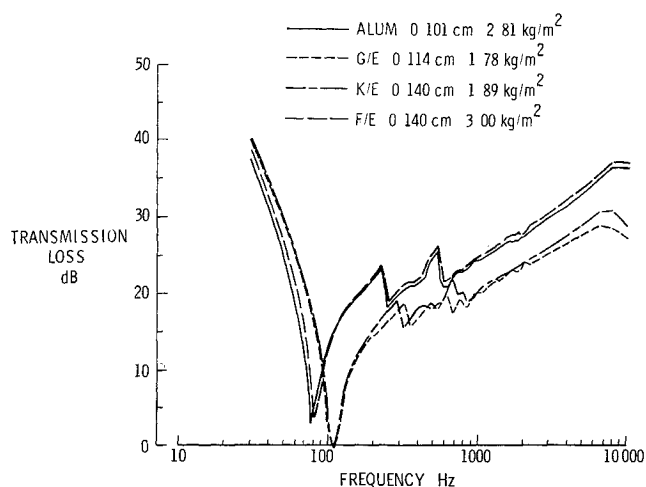


Fig 8 Finite panel theory transmission loss for design comparison of aluminum and composite panels

the boundary conditions of the panel. Thus, a finite panel transmission loss theory is needed. Such a theory has been developed and is currently being implemented. The theory models the test panel as a rectangular plate simply supported in an infinite baffle. Field incidence plane waves are assumed to impinge upon one side of the panel. The resulting panel vibrations are calculated by a normal mode approach with the plate properties assumed to be orthotropic. A Green's function integral equation is used to link the panel vibrations to the transmitted spherical sound waves. The incident and transmitted acoustic powers are calculated by integrating the incident and transmitted intensities over their appropriate areas, and transmission loss is calculated from the ratio of transmitted to incident acoustic power. The model has been implemented to the point of calculating oblique incidence transmission loss for a single plane acoustic wave impinging on the panel as compared to field incidence for many plane waves.

Calculations of fundamental frequencies and oblique incidence transmission loss have been performed to obtain preliminary data on the effects of composites on low frequency noise transmission. The equations for the fundamental frequencies of anisotropic simply supported and clamped plates have been presented by Bert¹⁰ and have been used here to calculate the fundamental frequencies of panels used in the present tests. These results are tabulated in Table 6. The angle orientation of the plies is seen to have a strong effect on the simply supported fundamental frequency for G/E and K/E tape panels. The +45/-45 deg configurations (GT1 or KT1) had about a 40% increase in fundamental frequency relative to the 0/90 deg configurations (GT2 or KT2). In comparing the fundamental frequencies of composite and aluminum design comparison panels, the G/E and K/E panels had about 40% higher frequencies than the aluminum panels (109 Hz compared to 79 Hz). In Fig 8 narrow band oblique incidence transmission loss, calculated with finite plate theory, has been plotted for the design comparison panels. Because of their higher fundamental frequencies, the G/E and K/E panels have over 12 dB more TL at the aluminum panel's resonance (79 Hz). The increase in TL over the aluminum panel is about 4 dB at the lowest frequencies plotted. Such transmission loss characteristics

indicate that composite materials may be beneficial for low frequency noise transmission problems at or below the resonance of conventional aluminum panels. For frequencies above the fundamental resonance region, the heavier aluminum panel has, in general, higher TL than the G/E or K/E panels; though at particular frequencies panel resonances cause the TL of the composite and aluminum panels to be about the same. Thus panel resonances can have an effect on frequencies normally considered to be in the mass controlled region.

Concluding Remarks

An experimental and theoretical research program has been initiated to develop an improved understanding of the noise transmission characteristics of composite materials. Such understanding is needed to ensure that the weight saving advantages of using composite materials in aircraft fuselage design are not compromised by high noise transmission. As a first step to see how composite structures will affect fuselage noise transmission relative to current aluminum structures, noise transmission tests have been conducted on large un-stiffened panels representative of the outer skin or inner trim panels. Concurrently, an analytical model for predicting the transmission loss of the test panels has been developed which allows for exact modeling of the anisotropic properties of the composite panels. The model is based on infinite panel theory and is applicable in the mass controlled and coincidence frequency regions. The regions of interest for the test panels. In comparing theory with measured data in the mass controlled region, good agreement, within 1 dB, was obtained. In the coincidence frequency region, agreement was also quite good with respect to the trend of transmission loss, even when the elastic properties used in the analysis were only isotropic estimates. In comparing composites with each other, the heavier panels, as expected, had the higher transmission loss in the mass controlled region, and the panels with the higher stiffness to mass ratios had the lower critical frequencies. The ply angle layup had no effect in the mass controlled region. Although the angle layup can affect the critical frequency, insufficient data was measured or calculated to determine the potential magnitude of the effect.

A theoretical design comparison between aluminum and composite panels based on equal critical shear load was also

conducted. This comparison indicated graphite/epoxy and Kevlar/epoxy panels to have 3 to 4 dB less transmission loss over most of the frequency range of interest due to their lighter weight and 6 to 12 dB less transmission loss at the highest frequencies of interest (up to 10 kHz) because of their lower critical frequencies.

In preparation for future tests to investigate the stiffness controlled frequency region, a finite panel field incidence transmission loss theory has been developed. The theory so far has been implemented for oblique incidence transmission loss. Preliminary calculations indicate that improved low frequency transmission loss might be possible with composite panels relative to conventional aluminum panels.

References

- ¹Davis G W and Sakata I F. Design Considerations for Composite Fuselage Structure of Commercial Transport Aircraft. NASA CR 159296, March 1981.
- ²Revell J D, Balena F J, and Koval L R. Analytical Study of Interior Noise Control by Fuselage Design Techniques on High Speed Propeller Driven Aircraft. NASA CR 159222, July 1978.
- ³Yang J C S and Tsui C Y. Optimum Design of Structures of Composite Materials in Response to Aerodynamic Noise and Noise Transmission. NASA CR 155332, Dec 1977.
- ⁴Koval L R. Sound Transmission into a Laminated Composite Cylindrical Shell. *Journal of Sound and Vibration*, Vol 71, No 4, 1980, pp 523-530.
- ⁵'Standard Method for Laboratory Measurement of Airborne Sound Transmission Loss of Building Partitions. ASTM Standard E90-75 in 1977 *Annual Book of ASTM Standards*, Part 18, American Society for Testing and Materials, Philadelphia, Pa.
- ⁶Grosveld F W, Characteristics of the Transmission Loss Apparatus at NASA Langley Research Center. NASA CR 172153, June 1983.
- ⁷Mixson J S, Roussos, L A, Barton C K, Vaicaitis R and Slazak, M. Laboratory Study of Add On Treatments for Interior Noise Control in Light Aircraft. *AIAA Journal of Aircraft*, Vol 20, June 1983, pp 516-522.
- ⁸Jones R M. *Mechanics of Composite Materials*. Scripta Book Company, Washington D C, 1975.
- ⁹Housner J M and Stein M. Numerical Analysis and Parametric Studies of the Buckling of Composite Orthotropic Compression and Shear Panels. NASA TN D 7996, Oct 1975.
- ¹⁰Bert C W. Design of Clamped Composite Material Plates to Maximize Fundamental Frequency. *Transactions of the ASME: Journal of Mechanical Design*, Vol 100, April 1978, pp 274-278.